Appl Phys A (2011) 103: 835–838
DOI 10.1007/s00339-010-6223-x

Applied Physics A
Materials Science & Processing

Influence of the group-velocity on the pulse propagation in 1D silicon photonic crystal waveguides

N.C. Panoiu · J.F. McMillan · C.W. Wong

Received: 15 January 2010 / Accepted: 3 December 2010 / Published online: 7 January 2011

Abstract We present a detailed analysis of the influence of the group velocity (GV) on the dynamics of optical pulses upon their propagation in one-dimensional photonic crystal waveguides (PhCW). The theoretical model used in our analysis incorporates the linear optical properties of the PhCW (GV dispersion and optical losses), free-carrier (FC) effects (FC dispersion and FC-induced optical losses) and nonlinear optical effects (Kerr nonlinearity and two-photon absorption). Our analysis shows that, unlike the case of uniform waveguides, the GV of the pulse, dispersion coefficients, and the waveguide nonlinear coefficient are periodic functions with respect to the propagation distance. We also demonstrate that linear and nonlinear effects depend on the group velocity, v_g, as v_g^{-1} and v_g^{-2}, respectively.

1 Introduction

Silicon photonics represents an emerging fast growing area of research, which is envisioned to revolutionize on-chip and chip-to-chip optical communications systems by developing silicon-based photonic devices manufactured using the well-established CMOS technology [1–3]. There are several unique properties of silicon that make it an ideal integration medium for functional photonic devices. For example, by using waveguides with a silicon core ($n_{Si} = 3.45$) and a low-index cladding ($n = 1$ for air and $n_{SiO_2} = 1.45$ for silica) one can achieve a very tight optical field confinement and, consequently, enhanced optical power flux. The second key optical property of silicon is an extremely large third-order susceptibility—about 3–4 orders of magnitude larger than that of silica. This large optical nonlinearity, in connection with the strong optical field confinement, leads to further enhancement of the effective optical nonlinearity of silicon-based photonic devices. This enhancement results in achieving strong nonlinear optical effects at low optical power [4], as well as very compact nonlinear optical devices [5–7]. In addition, for subwavelength waveguides both the linear dispersion coefficients [8, 9], as well as the nonlinear effective coefficient of the waveguide [3], depend chiefly on the geometry of the photonic structure.

One very promising approach to further decrease the size of silicon-based photonic systems is to employ nanostructured devices based on photonic crystals (PhCs). Thus, subwavelength patterning increases the device parameter space and therefore it provides an efficient approach to tailor and optimize the device functionality. For example, by simply tuning the geometrical parameters of PhC waveguides (PhCWs) one can achieve an optical guiding regime in which the group velocity (GV) of the propagating modes of the waveguide is as small as $10^{-4}c$ [10]. In this slow-light regime nonlinear optical effects, such as Raman interaction [11], third-harmonic generation [12, 13], and superprism effects [14], are dramatically enhanced and therefore the footprint of active devices can be reduced significantly. It is expected that, in addition, these enhanced nonlinear optical effects would strongly affect the dynamics of optical pulses propagating in subwavelength silicon waveguides. In this connection, in this paper we study the influence of the GV on the temporal and spectral characteristics of optical pulses propagating in PhCWs made of silicon.

N.C. Panoiu (✉)
Department of Electronic and Electrical Engineering, University College London, Torrington Place, London WC1E 7JE, UK
e-mail: n.panoiu@ee.ucl.ac.uk

J.F. McMillan · C.W. Wong
Optical Nanostructures Laboratory, Columbia University, New York, NY 10027, USA

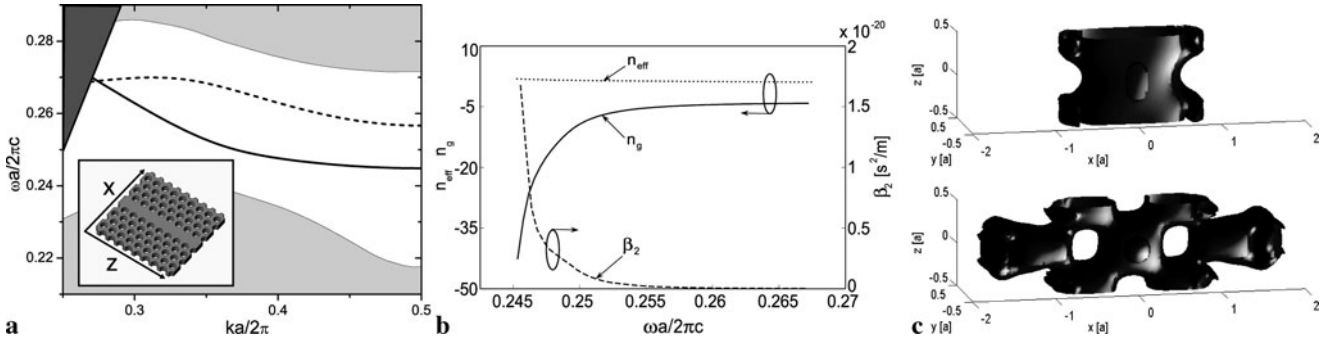

Fig. 1 (**a**) Projected band structure of a Si PhC slab waveguide with $h = 0.6a$ and $r = 0.22a$. *Solid* and *dashed curves* correspond to the fundamental and second mode, respectively. *Dark grey* and *light grey regions* correspond to leaky modes and slab guiding modes, respectively. (**b**) Dependence of n_{eff}, n_g, and β_2 on the normalized frequency, calculated for $a = 412$ nm. (**c**) Isosurface plots of the field intensity of a mode with $\tilde{\omega} = 0.267$ (*top panel*) and a slow-light mode with $\tilde{\omega} = 0.245$ (*bottom panel*)

2 Dispersion properties of the photonic crystal waveguide

To begin with, we consider a PhC slab waveguide with thickness h, made of silicon, perforated by a hexagonal lattice of holes; the lattice constant and hole radius are a and r, respectively. A one-dimensional (1D) waveguide is then obtained by filling one of the rows of holes, which is assumed to be oriented along the ΓK crystal symmetry axis [see Fig. 1(a)]. The coordinate system is chosen such that the line defect is oriented along the z-axis whereas the y-axis is perpendicular to the plane of the PhC slab. Then, the spatial distribution of the index of refraction is described by the function $n(\mathbf{r})$, where $n(\mathbf{r}) = 1$ and $n(\mathbf{r}) = n_{\text{Si}} \equiv n$ for the regions of the holes and outside the slab, and for the silicon regions, respectively.

We have determined the photonic band structure of the 1D PhC waveguide by using a numerical method based on the plane wave expansion algorithm. We have considered a PhCW with $h = 0.6a$ and $r = 0.22a$, and used a supercell with size of $6\sqrt{3}a \times 4a \times a$ along the x-, y-, and z-axis, respectively. The size of the computational step along the x, y, and z directions was $a\sqrt{3}/40$, $a/20$, and $a/20$, respectively. The results of our numerical simulations, presented in Fig. 1(a), show that the PhCW has two (TE-like) guiding modes located in the full frequency band gap of the PhC slab waveguide. Since the index of refraction $n(\mathbf{r})$ of the 1D PhCW is periodic along the z-axis, the Bloch theorem implies that the mode propagation constant, β, which is oriented along the z-axis, is restricted to the first Brillouin zone, $\beta \in [-\pi/a, \pi/a]$. Note also that the dispersion curves shown in Fig. 1(a) are given in dimensionless units, namely, $\tilde{\omega} = \frac{\omega a}{2\pi c}$ for the normalized frequency and $\tilde{k} = \frac{\beta a}{2\pi}$ for the normalized wave vector.

One important property of the guiding modes of the PhCW, which is illustrated in Fig. 1(c), is that the mode field profile is strongly dependent on the frequency, Therefore, one expects that the mode propagation constant varies strongly with the frequency. The dependence $\beta = \beta(\omega) \equiv \frac{n_{\text{eff}}\omega}{c}$, where n_{eff} is the effective index of the mode, allows us to determine a set of dispersion coefficients that characterize the optical pulse dispersion in the waveguide. Specifically, $\beta_1 \equiv \frac{\partial\beta}{\partial\omega} = \frac{1}{v_g}$ defines the GV of the optical pulse, whereas $\beta_2 \equiv \frac{\partial^2\beta}{\partial\omega^2}$ describes the pulse GV dispersion (GVD). The frequency dependence of these dispersion coefficients, calculated for the fundamental mode, is presented in Fig. 1(b). Among other things, this figure shows that near the edge of the first Brillouin zone the group index $n_g = c/v_g$ has large absolute value, one immediate consequence being that β_2 becomes very large in this slow-light regime.

3 Mathematical model

The theoretical model that describes the pulse propagation in 1D PhCWs, which has been derived in Ref. [15], consists of an equation that governs the evolution of the optical field,

$$i\left[\frac{\partial A}{\partial z} + \frac{\delta(z)}{v_g}\frac{\partial A}{\partial t}\right] - \frac{\beta_2\delta(z)}{2}\frac{\partial^2 A}{\partial t^2} = -\frac{\omega\delta n_{\text{FC}}}{n v_g}\kappa(z)A - i\frac{c\alpha_{\text{FC}}}{2n v_g}\kappa(z)A - \gamma(z)|A|^2 A, \quad (1)$$

coupled with a standard rate equation, which describes the FC dynamics,

$$\frac{\partial N(z,t)}{\partial t} = -\frac{N(z,t)}{\tau_c} + \frac{3\Gamma''(z)}{4\epsilon_0\hbar a^2 v_g^2 A_{nl}(z)}|A(z,t)|^4. \quad (2)$$

In these equations, $A(z,t)$ is the field amplitude (measured in $\sqrt{\text{W}}$), $N(z,t)$ is the FC density, τ_c is the FC relaxation time, δn_{FC} and α_{FC} are the FC-induced change in the index of refraction and the FC loss coefficient, respectively, and are proportional to the FC density N, A_{nl} is the effective

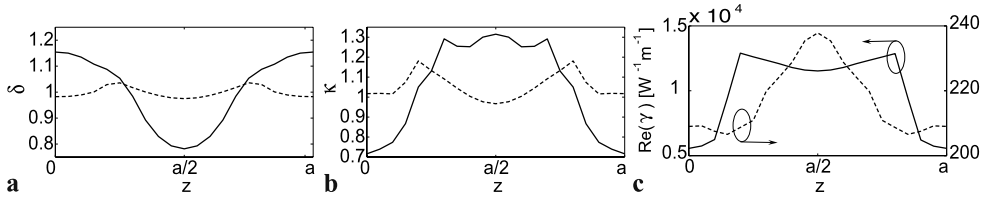

Fig. 2 The group-velocity shift δ, the mode overlap parameter κ, and waveguide nonlinear coefficient γ *vs*. distance z, calculated for the fast- and slow-light modes presented in Fig. 1(c). *Dashed* and *solid curves* correspond to the fast- and slow-light modes, respectively

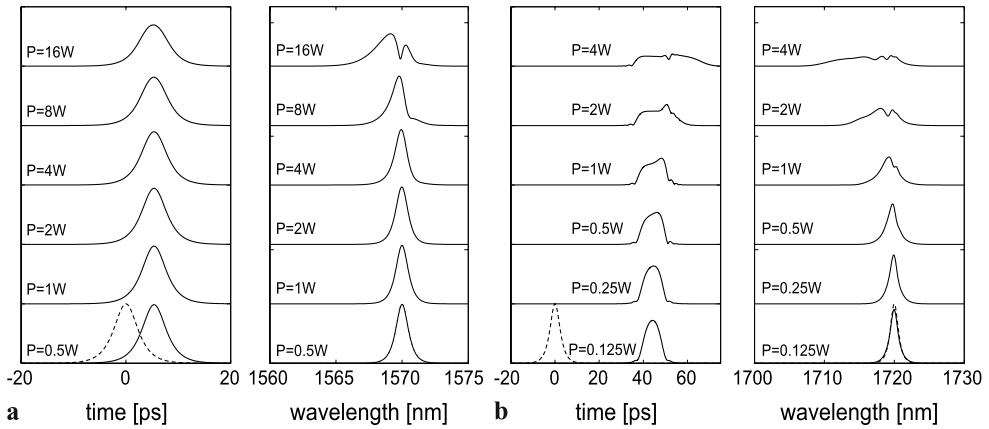

Fig. 3 (**a**) The temporal and spectral pulse profiles calculated for several values of power P. For a better illustration, the pulse profiles are displaced vertically by a constant shift. The pulse GV $v_g = c/4.125$, which corresponds to $\tilde{\omega} = 0.267$. The PhCW has $h = 0.6a$ and $r = 0.22a$, with $a = 421$ nm. The pulse width $T_0 = 2$ ps, $\beta_2 = 10$ ps^2/m, and the propagation distance $z = 1000a$. (**b**) The same as in (**a**), but for a slow-light mode with $v_g = c/35$, $\tilde{\omega} = 0.245$, and $\beta_2 = 10^4$ ps^2/m. The *dashed curves* correspond to the input pulse

area of the mode, and

$$\gamma(z) = \frac{3\omega\Gamma(z)}{4\epsilon_0 a^2 v_g^2} \tag{3}$$

is the nonlinear coefficient of the waveguide. Furthermore, the averaged third-order susceptibility, Γ, the GV shift, δ, and the mode overlap coefficient, κ, are given by the following expressions:

$$\Gamma(z) = \frac{a^4 \int \mathbf{e}^* \cdot \hat{\chi}^{(3)} \vdots \mathbf{eee}^* \, dS}{\int_{V_{\text{cell}}} n^2(\mathbf{r}) |\mathbf{e}|^2 \, dV};$$

$$\delta(z) = \frac{a \int [\mu_0 |\mathbf{h}|^2 + n^2(\mathbf{r}) |\mathbf{e}|^2] \, dS}{\int_{V_{\text{cell}}} [\mu_0 |\mathbf{h}|^2 + n^2(\mathbf{r}) |\mathbf{e}|^2] \, dV};$$

$$\kappa(z) = \frac{an^2 \int_{S_{nl}} |\mathbf{e}|^2 \, dS}{\int_{V_{\text{cell}}} n^2(\mathbf{r}) |\mathbf{e}|^2 \, dV}, \tag{4}$$

where $\hat{\chi}^{(3)}$ is the third-order susceptibility of bulk silicon and $\mathbf{e}(\mathbf{r})$ and $\mathbf{h}(\mathbf{r})$ are the electric and magnetic field of the waveguide mode, respectively. It should be noted that, as shown in Fig. 2, and unlike the case of uniform waveguides, these physical quantities are periodic functions of the distance z. Figure 2 also shows that this dependence on z is much stronger in the case of the slow-light mode as compared to the case of the fast-light mode, which emphasizes the strong frequency dispersion of these PhCWs.

4 Influence of group velocity on pulse dynamics

One important conclusion illustrated by the (1) and (2) is that the GV of the optical pulse would have a strong influence on the pulse dynamics, especially at large peak power, P. To be more specific, the linear terms in the (1) are inverse proportional to v_g, which implies that the FC-induced losses are inverse proportional to v_g, whereas the nonlinear terms in the (1) and (2) are inverse proportional to v_g^2. In other words, when compared to the fast-light regime, in the slow-light regime the nonlinear optical effects are enhanced significantly more than the linear ones. This dependence, however, becomes more complicated as the power increases, since in this case the generated FCs increase the linear and nonlinear absorption *via* the FC absorption and two-photon absorption (TPA), respectively. Thus, as can be seen from the (2), the amount of FCs generated *via* TPA is inverse proportional to v_g^2, and therefore the FC-induced losses become inverse proportional to v_g^3.

In order to illustrate this strong dependence of the pulse dynamics on the GV, we present in Fig. 3 the temporal and spectral profiles of a pulse that propagates in a silicon PhCW, both in the fast-light and the slow-light regimes. In these numerical simulations the spatial integration step was $a/20$ and the relaxation time $\tau_c = 0.5$ ns. In both cases the pulse temporal width $T_0 = 2$ ps and the propagation distance $z = 1000a$ are the same. Among other things, this figure shows that in the fast-light regime the temporal profile of the pulse remains almost unchanged during the propagation, except for a small decrease in amplitude due to the FC losses and TPA. On the other hand, it can be seen that at large optical power the spectrum of the pulse becomes asymmetric and splits in two separate pulses, the latter feature being the signature of the self-phase modulation effect. By contrast, in the slow-light regime both the temporal profiles of the pulse, as well as the pulse spectra, are modified dramatically during the pulse propagation in the waveguide. Specifically, because in this case β_2 is three orders of magnitude larger than in the fast-light regime, the temporal width of the pulse broadens significantly. Moreover, even at moderate optical power the pulse decay is much stronger in this case, which means that the optical losses due to the generation of FCs and TPA are larger. Note also that in the slow-light regime the spectrum of the pulse develops a series of oscillations, which again is a signature of the phase modulation induced by the FC dispersion and the Kerr effect. Indeed, the nonlinear coefficient γ of the slow-light mode is about two orders of magnitude larger than in the case of the fast mode, and therefore in this case one expects that the pulse is much more strongly influenced by the increased amount of generated FCs and the enhanced nonlinear optical effects.

5 Conclusion

In conclusion, we have presented a detailed analysis of the influence of the GV on the pulse propagation in 1D PhCWs made of silicon. In particular, we have included in our analysis linear optical effects induced by the waveguide dispersion and nonlinear optical effects due to the (Kerr) nonlinearity of silicon, and studied their influence on the pulse propagation. We have applied the general theoretical formalism to two particular cases, namely, the propagation of optical pulses in a single mode PhCW in the slow-light and fast-light regimes. One important conclusion of this theoretical analysis is that due to a complex interplay between effects induced by the generation of FCs and nonlinear optical effects, the pulse dynamics in the slow-light and fast-light regimes show markedly different physical characteristics.

Acknowledgement This work was supported by the UK Engineering and Physical Sciences Research Council (EPSRC), grant no. EP/G030502/1.

References

1. G.T. Reed, A.P. Knights, *Silicon Photonics: An Introduction* (Wiley, New York, 2004)
2. Q. Lin, O.J. Painter, G.P. Agrawal, Nonlinear optical phenomena in silicon waveguides: Modeling and applications. Opt. Express **15**, 16604–16644 (2007)
3. R.M. Osgood, N.C. Panoiu, J.I. Dadap, X. Liu, X. Chen, I.-W. Hsieh, E. Dulkeith, W.M.J. Green, Y.A. Vlasov, Engineering nonlinearities in nanoscale optical systems: physics and applications in dispersion-engineered silicon nanophotonic wires. Adv. Opt. Photon. **1**, 162–235 (2009)
4. E. Dulkeith, Y.A. Vlasov, X. Chen, N.C. Panoiu, R.M. Osgood, Self-phase-modulation in submicron silicon-on-insulator photonic wires. Opt. Express **14**, 5524–5534 (2006)
5. R. Claps, D. Dimitropoulos, V. Raghunathan, Y. Han, B. Jalali, Observation of stimulated Raman amplification in silicon waveguides. Opt. Express **11**, 1731–1739 (2003)
6. H. Rong, A. Liu, R. Jones, O. Cohen, D. Hak, R. Nicolaescu, A. Fang, M. Paniccia, An all-silicon Raman laser. Nature **433**, 292–294 (2005)
7. I.-W. Hsieh, X. Chen, J.I. Dadap, N.C. Panoiu, R.M. Osgood, S.J. McNab, Y.A. Vlasov, Crossphase modulation-induced spectral and temporal effects on co-propagating femtosecond pulses in silicon photonic wires. Opt. Express **15**, 1135–1146 (2007)
8. X. Chen, N.C. Panoiu, R.M. Osgood, Theory of Raman-mediated pulsed amplification in silicon-wire waveguides. IEEE J. Quantum Electron. **42**, 160–170 (2006)
9. A.C. Turner, C. Manolatou, B.S. Schmidt, M. Lipson, M.A. Foster, J.E. Sharping, A.L. Gaeta, Tailored anomalous group-velocity dispersion in silicon channel waveguides. Opt. Express **14**, 4357–4362 (2006)
10. M. Soljacic, S.G. Johnson, S. Fan, M. Ibanescu, E. Ippen, J.D. Joannopoulos, Photonic-crystal slow-light enhancement of nonlinear phase sensitivity. J. Opt. Soc. Am. B **19**, 2052–2059 (2002)
11. J.F. McMillan, X. Yang, N.C. Panoiu, R.M. Osgood, C.W. Wong, Enhanced stimulated Raman scattering in slow-light photonic crystal waveguides. Opt. Lett. **31**, 1235–1237 (2006)
12. M. Bahl, N.C. Panoiu, R.M. Osgood, Nonlinear optical effects in a two-dimensional photonic crystal containing one-dimensional Kerr defects. Phys. Rev. E **67**, 056604 (2003)
13. B. Corcoran, C. Monat, C. Grillet, D.J. Moss, B.J. Eggleton, T.P. White, L. O'Faolain, T.F. Krauss, Green light emission in silicon through slow-light enhanced third-harmonic generation in photonic crystal waveguides. Nat. Photon. **3**, 206–210 (2009)
14. N.C. Panoiu, M. Bahl, R.M. Osgood, Optically tunable superprism effect in nonlinear photonic crystals. Opt. Lett. **28**, 2503–2505 (2003)
15. N.C. Panoiu, J.F. McMillan, C.W. Wong, Theoretical analysis of pulse dynamics in silicon photonic crystal wire waveguides. IEEE J. Sel. Top. Quantum Electron. **16**, 257–266 (2010)